Molecular and Cellular Biology

Complementary Roles of Yeast Rad4p and Rad34p in Nucleotide Excision Repair of Active and Inactive rRNA Gene Chromatin

Maxime Tremblay, Yumin Teng, Michel Paquette, Raymond Waters and Antonio Conconi

Updated information and services can be found at:
http://mcb.asm.org/content/28/24/7504

These include:

REFERENCES	This article cites 61 articles, 30 of which can be accessed free at: http://mcb.asm.org/content/28/24/7504#ref-list-1
CONTENT ALERTS	Receive: RSS Feeds, eTOCs, free email alerts (when new articles cite this article), more»

Information about commercial reprint orders: http://journals.asm.org/site/misc/reprints.xhtml
To subscribe to to another ASM Journal go to: http://journals.asm.org/site/subscriptions/

Journals.ASM.org

Vol. 28, No. 24

Complementary Roles of Yeast Rad4p and Rad34p in Nucleotide Excision Repair of Active and Inactive rRNA Gene Chromatin[▽]

Maxime Tremblay,[1]† Yumin Teng,[2]† Michel Paquette,[1] Raymond Waters,[2] and Antonio Conconi[1]*

Département de Microbiologie et d'Infectiologie, Faculté de Médecine, Université de Sherbrooke, Sherbrooke, Quebec J1H 5N4, Canada,[1] and Department of Pathology, School of Medicine, Cardiff University, Health Park, Cardiff CF14 4XN, United Kingdom[2]

Nucleotide excision repair (NER) removes a plethora of DNA lesions. It is performed by a large multisubunit protein complex that finds and repairs damaged DNA in different chromatin contexts and nuclear domains. The nucleolus is the most transcriptionally active domain, and in yeast, transcription-coupled NER occurs in RNA polymerase I-transcribed genes (rDNA). Here we have analyzed the roles of two members of the xeroderma pigmentosum group C family of proteins, Rad4p and Rad34p, during NER in the active and inactive rDNA. We report that Rad4p is essential for repair in the intergenic spacer, the inactive rDNA coding region, and for strand-specific repair at the transcription initiation site, whereas Rad34p is not. Rad34p is necessary for transcription-coupled NER that starts about 40 nucleotides downstream of the transcription initiation site of the active rDNA, whereas Rad4p is not. Thus, although Rad4p and Rad34p share sequence homology, their roles in NER in the rDNA locus are almost entirely distinct and complementary. These results provide evidences that transcription-coupled NER and global genome NER participate in the removal of UV-induced DNA lesions from the transcribed strand of active rDNA. Furthermore, nonnucleosome rDNA is repaired faster than nucleosome rDNA, indicating that an open chromatin structure facilitates NER in vivo.

Nucleotide excision repair (NER) removes lesions from DNA such as the UV photoproducts *cis-syn* cyclobutane pyrimidine dimer (CPD) and pyrimidine (6-4) pyrimidone. The NER pathway involves damage recognition, incision of the DNA strand containing the damage, excision of the lesion, and repair synthesis (16, 43). In addition, CPDs are rapidly eliminated from the transcribed strand (TS) of active RNA polymerase II (RNAPII)-transcribed genes, a process that is referred to as transcription-coupled NER (TC-NER) (3, 29, 34, 35, 45). In *Saccharomyces cerevisiae*, mutations in the *RAD26* gene affect TC-NER (55) but not repair of the nontranscribed regions of the genome, or global genome NER (GG-NER). The GG-NER requires the Rad7p/Rad16p and Abf1p complexes (16, 43).

Much research has been devoted to elucidating the roles of Rad4p. For instance, it was found that deletion of *RAD4* causes the DNA incision step to be completely defective, that Rad4p is required for NER in vitro, and that binding of Rad4p (and Rad2p) to TFIIH defines intermediates during the assembly of NER proteins at sites of DNA damage (2, 23, 43, 63). Therefore, it is suggested that the Rad14p/Rad4p-Rad23p complex locates the DNA lesions and promotes assembly of the repair machinery at these sites (22, 23, 24, 28). During this process, Rad4p first binds undamaged DNA sequences, and then it repositions at the 3′ side of the lesion and induces a flipout of the damaged base from the DNA helix (38, 48). The Rad4 protein works in complex with Rad23p, which has a

ubiquitin-like domain and supports interactions with the 19S regulatory particle of the 26S proteasome. The ubiquitin proteasome pathway plays important roles in NER via both proteolytic and nonproteolytic activities (19, 44, 65). The xeroderma pigmentosum group C (XPC) gene is the human counterpart of *RAD4*. However, whereas Rad4p is required for the incision step in both GG-NER and TC-NER, the XPC protein is required only for GG-NER (57, 58). This led to the hypothesis that XPC makes compact chromatin accessible to NER. To investigate this possibility, the activity of XPC was analyzed on nucleosome DNA. In one study, it was observed that the addition of undamaged, naked DNA to in vitro NER reaction mixtures hampers XPC binding to photoproducts. Conversely, no inhibitory effect occurs when the undamaged carrier DNA is wrapped into nucleosomes, suggesting that the presence of nucleosomes in undamaged DNA endorses the specificity of XPC for damaged sites (65a). Another study showed that binding of XPC to DNA lesions is hindered when the lesions are positioned within nucleosome DNA (26). Finally, a recent report has shown that Rad4p-Rad23p copurifies with two subunits of the SWI/SNF chromatin-remodeling complex. Since UV stimulates this interaction, it is proposed that Rad4-Rad23p recruits the SWI/SNF chromatin-remodeling complex to DNA lesions, which enhances the accessibility for NER to nucleosome DNA (20). In summary, the Rad4p/XPC group of proteins appears to have multiple functions, which could be affected by factors like transcription rate, chromatin structure, and the subregions of the nucleus that undergo repair. Moreover, while Rad4p is considered indispensable for the repair of UV-damaged DNA (43), a series of in vitro assays have shown that repair of DNA lesions in locally unwound DNA can take place in the absence of XPC (40).

The nucleolus is a defined region that is made of clusters of ribosomal genes (rRNA genes [rDNA]). The rRNA genes are

* Corresponding author. Mailing address: Département de Microbiologie et Infectiologie, Faculté de Médecine, Poste 7446, Université de Sherbrooke, 3001 12th Ave. Nord, Sherbrooke, QC J1H 5N4, Canada. Phone: (819) 564-5360. Fax: (819) 564-5392. E-mail: antonio.conconi@usherbrooke.ca.
† These authors contributed equally.

heavily transcribed by RNA polymerase I (RNAPI) (39) and are present in multiple copies (~150 in yeast [42]) of two coexisting and distinct types forming total rDNA. One type is permissive to transcription, and the other type is transcriptionally refractive (11, 12, 13, 21). Canonical nucleosomes are absent from the coding regions of ribosomal genes that are permissive to transcription (open rDNA), whereas nucleosomes are present on the inactive genes (closed rDNA) (30, 47). Also, nucleosomes are found on most of the DNA sequences flanking the rDNA units (or intergenic spacers [IS]) (30, 47, 61). In contrast to human cells, yeast cells rapidly remove CPDs from rDNA (7, 8). Furthermore, strand-specific repair was observed for rDNA of the rad7Δ and rad16Δ mutants (59), and TC-NER was measured in the active rDNA fraction of wild-type (WT) cells (7, 10, 33). Although NER was analyzed in total rDNA and important results were reported (14, 15, 59), a number of questions remain unanswered because those studies did not follow NERs separately in the active and inactive rDNA. Namely, in the rad4Δ mutant, about half of all CPDs in the TS of total rDNA are repaired, whereas no repairs occur in the rest of the genome, including the nontranscribed strand (NTS) of total rDNA (59). In spite of the fact that this observation was not explained, the role of Rad4p in the repair of RNAPI-transcribed rDNA is more akin to the role of Rad7/Rad16 in the repair of RNAPII-transcribed genes and to the role of XPC in the repair of RNAPII-transcribed genes in human cells. Also, YDR314C (renamed Rad34p) shares sequence homology with Rad4p (31). It interacts with Rad23p (18) and is involved in repair of rDNA, but it does not participate in NER of RNAPII-transcribed genes (14). The function of Rad34p was investigated using the rad16Δ mutant as a background strain, and NER was measured in the rad16Δ versus the rad16Δ rad34Δ double mutant (14). It was found that in the double mutant, there is no preferential repair of the rDNA TS, suggesting that Rad34p could be involved in TC-NER. However, as stated by the authors of that study (14), those experiments have not shown that such Rad34p-dependent preferential repair occurs only in the active rDNA. Consequently, the possibility that the Rad34-dependent repair in rad16Δ cells is, in fact, RNAPI transcription independent could not be excluded. Hence, participation of the Rad34p in TC-NER of rDNA was not definitively shown (14).

Psoralen cross-linking has been employed to separate the two forms of rDNA and to study the structure of chromatin during transcription, replication, and repair (47, 53). In this report, psoralen cross-linking was used to verify that the active rDNA is preferentially released when nuclei are digested with restriction enzymes. Thereafter, active and inactive rDNA were separated, and NER was followed in both rDNA populations of the WT, rad4Δ, rad34Δ, and rad4Δ rad34Δ cells. The rates of NER in the active and inactive rDNA chromatin of the coding regions were measured relative to the rates of NER in the mostly nontranscribed IS, which are organized in nucleosomes. In addition, CPD removal was analyzed at the nucleotide level in the promoter region and around the RNAPI transcription initiation site. These experiments were undertaken to identify the boundaries between regions where Rad4p and Rad34p promote repair, to determine whether they have complementary or redundant functions, and to compare TC-NER with RNAPI transcription elongation.

MATERIALS AND METHODS

Yeast cells and UV irradiation. *S. cerevisiae* (strain JS311 [*RAD*$^+$] [46]) was grown in yeast extract peptone dextrose medium to early log phase (optical density at 600 nm of 0.4; ~1.2 × 10^7 cells/ml). The isogenic rad4Δ, rad34Δ, and rad4Δ rad34Δ strains were constructed by PCR-mediated gene disruption as previously described (1). Cultures were harvested by centrifugation, washed in ice-cold phosphate-buffered saline (137 mM NaCl, 2.5 mM KCl, 2 mM KH$_2$PO$_4$, 10 mM Na$_2$HPO$_4$ [pH 7.0]), and resuspended in the same buffer to 2 × 10^7 cells/ml. Cell suspensions were poured into trays to ~2-mm depth and irradiated (primary, 254 nm) with 180 J/m^2 of UV (UVX radiometer; Ultra-Violet Products, Upland, CA). Then, cells were harvested, resuspended in yeast extract peptone dextrose medium, and incubated in the dark at 30°C with continuous shaking for the indicated repair times (see Results).

Nucleus isolation and DNA extraction. Cells (~1.6 × 10^9) were collected, washed with ice-cold phosphate-buffered saline, resuspended in 1.5 ml of ice-cold nucleus isolation buffer (NIB) (50 mM morpholinepropanesulfonic acid [pH 8.0], 150 mM potassium acetate, 2 mM MgCl$_2$, 17% glycerol, 0.5 mM spermine, and 0.15 mM spermidine), and transferred to 15-ml polypropylene tubes containing 1.5 ml of glass beads (425- to 600-μm diameter; Sigma). Cells were disrupted by vortexing by using 16- to 30-s pulses with 30-s pauses on ice. Nuclear suspensions were collected, and the glass beads were rinsed twice with 1 ml of NIB. The combined suspensions were centrifuged as previously described (7, 10). Nuclei were resuspended in 800 μl of NIB and stored in 200-μl aliquots at −80°C in the dark.

To measure repair of the individual strands of active and inactive rDNA, nuclei were pelleted, resuspended in 0.5 ml of EcoRI restriction enzyme buffer, and digested according to the manufacturer's recommendations (New England BioLabs). DNA from EcoRI-digested nuclei was extracted as described below, resuspended in NheI buffer, and digested according to the manufacturer's recommendations (New England BioLabs). All steps were carried out under gold light (reprographic gold; Standard Products Inc.). In parallel, aliquots of EcoRI-digested nuclei were photo cross-linked with psoralen to monitor the separation of active from inactive rDNA, as previously described (7, 10).

To measure NER in total rDNA, DNA was extracted from cells broken by vortexing in the presence of glass beads, as described above. To each 200-μl aliquot was added 300 μl of TE buffer, 225 μl of 3 M Na-acetate, and 35 μl of 10% sodium dodecyl sulfate. After two extractions with phenol-chloroform (1:1) and one extraction with chloroform, nucleic acids were precipitated in isopropanol. Following centrifugation, pellets were dissolved in TE buffer, treated with RNase (Roche), phenol extracted, and precipitated in ethanol. DNA was resuspended in TE and digested with the appropriate restriction enzymes, as described in Results.

T4 endonuclease digestion, alkaline gel electrophoresis, Southern blotting, and quantification of CPD yield. DNA samples were cleaved at CPDs by T4 endonuclease V (T4 endo V; Epicentre) according to the manufacturer's recommendations. After T4 endo V digestion, ~5 μg of DNA per sample was separated by 1% alkaline agarose gel electrophoresis (7, 10). DNA was transferred to Hybond-XL membranes (GE Healthcare) in 0.4 N NaOH. Radioactive probes (Fig. 1A, upper panel) were generated using random primers or strand-specific riboprobe kits (Promega), and hybridization and washing were carried out at 65°C as previously described (11). Filter membranes were exposed to phosphorimager screens (Molecular Dynamics), and CPDs were quantified from phosphor images of the Southern blots, using ImageQuant software (Molecular Dynamics). Measurement of CPDs in each strand of rDNA was performed as previously described (7, 10).

High-resolution mapping of the CPD sites. Measuring CPDs in the individual strands at nucleotide resolution was carried out as previously described (50). DNA was digested with HhaI at 37°C for 1 h in a total reaction mixture volume of 200 μl, generating a 768-bp fragment covering an upstream region (266 bp) and part of the coding region (502 bp) of the 35S rRNA gene (Fig. 1A, upper panel). After phenol-chloroform extraction, DNA was precipitated using 20 μl of Na acetate (3 M) and 220 μl of isopropanol. Then, DNA pellets were resuspended in 100 μl of TE buffer and cleaved specifically at CPDs, using T4 endo V as described above. After phenol-chloroform and chloroform extraction, damage in the TS was detected by adding 1 pmol of biotinylated probe 1 (5′-biotin-GATAGCTTTTTTCGCGTTTCCGTATTTTCCGCTTGG) to the samples. The DNA samples were denatured at 95°C for 5 min and then incubated at 55°C for 15 min to allow probe annealing to rDNA fragments. (The length of the fragments annealed to the probe depends on the positions of CPDs within the
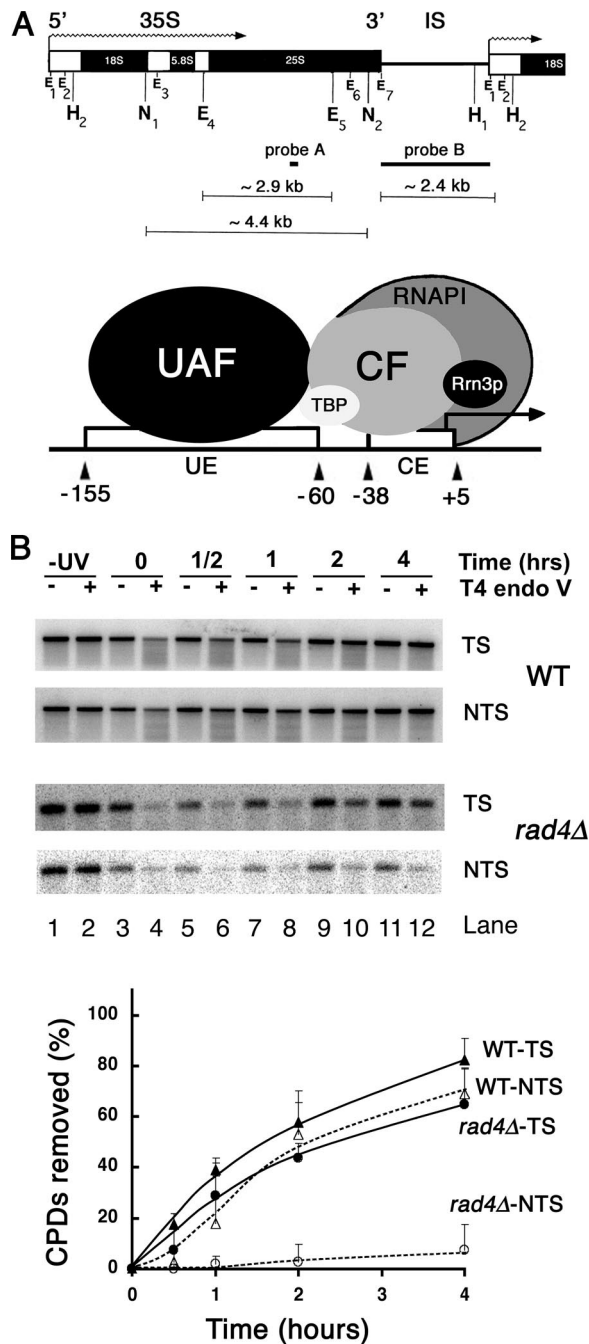
FIG. 1. (A) The upper panel shows a map of the yeast 35S rRNA gene. The gene, its 5′ and 3′ ends, and the direction of transcription (wavy arrow) are shown. Black boxes represent the probes (A, ~140 bp; B, ~2.4 kb). E_1 to E_7 mark the positions of the seven EcoRI restriction sites, N_1 and N_2 mark the positions for the two NheI restriction sites, and H_1 and H_2 mark the positions for the two HhaI sites used in this study (in the rDNA locus there are 16 HhaI sites). (A) The lower panel shows that in yeast, transcription initiation entails the interaction of at least four transcription factors, with the promoter elements UE (upstream element) and CE (core element). UAF (upstream activating factor), CF (core factor), TBP (TATA-box binding protein), and Rrn3p bind RNAPI. DNase I footprinting was shown for UAF (nucleotides −160 to −50) and CF (nucleotides −45 to +1) (4, 61). The arrow shows the direction of transcription, and position +1 is the site of transcription initiation (39, 42). (B) Repair of CPDs in the coding region of total rDNA, in the WT and *rad4Δ* cells. Cells

fragment.) Next, 100 μg of washed streptavidin-coated Dynabeads M-280 (Invitrogen) was added to samples, mixed, and kept at room temperature for 15 min to allow binding of the streptavidin-coated Dynabeads to the biotin molecule at the 5′ end of the probe. The rDNA fragments were purified with a Dynal magnetic particle concentrator. The supernatant containing the NTS fragments (and the rest of the genomic DNA) was removed and kept for purification of the NTS. The NTS of rDNA fragments was purified as performed for the TS, except that probe 2 (5′-biotin-GATAGCTTTTTTCFCACTCCGTCACCATACCATA GCA) was used. The beads were washed with 50 μl of washing buffer (5 mM Tris-HCl [pH 7.5], 0.5 mM EDTA, 1.0 M NaCl) at 55°C for 5 min, and then the buffer was removed. Two more washes were done with 50 μl of H_2O at room temperature. Then, rDNA fragments were end labeled with six [α-^{32}P]dATP residues by T7 DNA polymerase (Amersham), which uses the six-T overhang of the probes as template (as described in reference 50). The reaction was complete after 10 min at 37°C, and the Dynabeads were washed twice with 30 μl of TE. Finally, the labeled rDNA fragments were eluted from the Dynabeads at room temperature by the addition of 3 μl of formamide loading buffer (95% formamide, 20 mM EDTA, 0.05% bromophenol blue) and separated by length by 6% denaturing polyacrylamide gel electrophoresis. The running buffer was TBE (89 mM Tris base, 89 mM boric acid, 2.5 mM $Na_2EDTA \cdot 2H_2O$), and electrophoresis was carried out at 40 V/cm. Gels were exposed to phosphorimager screens, and CPD quantification in rDNA was performed from the phosphor images, using Image-Quant software as described previously (52).

RESULTS

Removal of CPDs from the coding regions of total rDNA is considerably reduced in *rad4Δ* cells. We first examined NER of total rDNA. At different times after irradiation, DNA was isolated from the WT and *rad4Δ* cells, digested with EcoRI, and treated with T4 endo V. Thereafter, DNA repair was measured by denaturing gel electrophoresis and Southern blotting as described previously (3). Typical images are shown in Fig. 1B (upper panel), where bands correspond to the ~2.9-kb fragment that is released from the central portion of the rDNA transcription unit (Fig. 1A, E_4 to E_5). After incubation with T4 endo V, changes in signal intensities of the EcoRI bands (compare − with + lanes) reflect the number of strand breaks at the CPDs. The data show that in the WT, both TS and NTS are repaired, whereas in the *rad4Δ* cells, repair occurs only in the TS (Fig. 1, compare lanes 5 to 12 with lanes 3 and 4). Quantitative analyses (Fig. 1B, lower panel) indicate that in the WT, ~ 80% of CPDs are removed from both DNA strands during the 4-h repair. For the *rad4Δ* cells, ~60% of CPDs are repaired from the TS, whereas no repair is observed for the NTS. Thus, the time courses for CPD removal measured in the yeast strains used in this study can be directly compared with those reported in reference 59.

In the absence of Rad4p, repair of individual DNA strands from active and inactive rDNA is unevenly affected. Determination of the efficiency of strand-specific repair in total rDNA by the Southern blot assay (as described above) is incomplete because data represent an average of active and inactive rDNA

were irradiated with 180 J/m^2 and harvested at the times indicated (h). Total DNA was purified, digested with EcoRI, treated with T4 endo V, and separated on 1% alkaline agarose gels. After blotting, filters were hybridized with strand-specific riboprobes-A (as shown in panel A). (B) The upper panel shows a representative phosphor image for the TS and the NTS of the WT and *rad4Δ* cells. (B) The lower panel shows quantification of the phosphor images. DNA repair is expressed as the percentage of CPDs removed versus repair time (h). Data are the means of three independent experiments.

copies. Accurate measurements are obtained when the two forms are separated and repair is followed individually for the active and inactive rDNA populations. To do so, nuclei were isolated from yeast harvested at the specified repair times and then digested with EcoRI (Fig. 1A, upper panel). Restriction enzyme digestions of nucleus release only active rDNA because nucleosomes are absent from these genes, making them accessible to endonucleases (7, 10, 41). Thereafter, DNA was purified and redigested with NheI (Fig. 1A, upper panel). Because the two EcoRI sites are within the NheI sites, a full-length fragment (~4.4 kb) obtained after NheI digestion of DNA isolated from EcoRI-treated nuclei contains primarily inactive rDNA. This double digestion allows following DNA repair in the inactive rDNA (NheI; see Fig. 2, i band) and in the active rDNA (EcoRI; see Fig. 2, a band) on the same filter membrane as previously described (7, 10). Psoralen photo cross-linking was used to monitor the separation of the two rDNA populations (data not shown; 7, 10).

In the WT and $rad4\Delta$ cells, at 180 J/m^2, the average yield $\pm$ standard deviation of CPDs/kb in the TS was 0.37 ± 0.04 and in the NTS was 0.32 ± 0.05. Representative data showing T4 endo V analyses for the TS and NTS of active and inactive rDNA are presented in Fig. 2A and B. The percentage of CPDs removed are given in Fig. 2E (WT and $rad4\Delta$ cells). For the WT, repair is significantly faster in the TS of active rDNA than in the NTS of the same fraction (Fig. 2, WT and compare TS a and NTS a). During the first 2 h, more than twice as many CPDs are removed from the TS as from the NTS. The process of TC-NER does not occur in the inactive rDNA, and there are no differences in repair rates between the TS and NTS (Fig. 2, WT and compare TS i and NTS i). Furthermore, CPDs are removed faster from the active rDNA than from the inactive rDNA chromatin. Also, the repair rate of active rDNA chromatin is initially high but rapidly levels off during removal of the remaining ~20% of CPDs. Conversely, removal of CPD from inactive rDNA chromatin occurs at a more uniform and lower rate throughout the entire repair time. For the $rad4\Delta$ cells, DNA repair in the TS of active rDNA (Fig. 2, TS a) is very rapid, complete within 2 h and faster than in the WT. On the contrary, DNA repair in the NTS of active rDNA is drastically reduced; only ~20% of the total CPDs are removed (Fig. 2, NTS a). Finally, very little or no repair was measured in the TS and NTS of inactive rDNA (Fig. 2, TS i and NTS i).

Lack of Rad34p affects repair in the transcribed strand of active, nonnucleosomal rDNA. To gain further insights into NER in RNAPI-transcribed genes, nuclei were isolated from the $rad34\Delta$ and $rad4\Delta$ $rad34\Delta$ cells before and after UV exposure. Nuclei were incubated with EcoRI, and the purified DNA was redigested with NheI and processed as described above. In the $rad34\Delta$ and $rad4\Delta$ $rad34\Delta$ cells, the yields of CPDs for the active and inactive rDNA fractions, TS and NTS, were as in the WT (see description above). Representative images of these experiments, showing repair analyses for the TS and NTS of active and inactive rDNA, are shown in Fig. 2C and D. The data, expressed as the percentage of CPDs removed over time, are shown in Fig. 2E ($rad34\Delta$ and $rad4\Delta$ $rad34\Delta$ cells).

For the $rad34\Delta$ cells, repair in the TS of active rDNA is reduced to the rate measured in the NTS (Fig. 2E, compare WT and $rad34\Delta$, TS a and NTS a). Therefore, TC-NER is abolished in the $rad34\Delta$ cells (Fig. 2E, $rad34\Delta$, compare TS a

and NTS a). In contrast, DNA repair in the NTS of active rDNA is only slightly affected, on average, ~15% less efficient than in the WT. Finally, repair of the inactive rDNA chromatin is unaffected in the $rad34\Delta$ cells (Fig. 2E, compare WT and $rad34\Delta$, TS i and NTS i), it is uniform, and it proceeds at a low rate. For the $rad4\Delta$ $rad34\Delta$ cells, repair is entirely abolished in both DNA strands and rDNA fractions (Fig. 2E, $rad4\Delta$ $rad34\Delta$).

Repair of the nucleosomal IS between rDNA units is affected in $rad4\Delta$ but not in $rad34\Delta$ cells. In the absence of Rad4p, inactive DNA and both strands of RNAPII-transcribed genes are not repaired (59, 60). On the other hand, CPDs are rapidly removed from the TS of active rDNA (see description above). To determine whether the redundancy of Rad4p is unique to DNA sequences that are loaded with RNAPI, DNA repair was followed in the IS between rDNA units (Fig. 1A, upper panel). The WT and $rad4\Delta$ cells were irradiated and incubated for different repair times, and the DNA was isolated and digested with EcoRI and prepared for the T4 endo V assay as described in Materials and Methods. Representative Southern blots are shown in Fig. 3A (WT and $rad4\Delta$ cells), where the EcoRI band represents almost and only the entire IS region (Fig. 1A, E_7 to E_1). The changes in signal intensities of the EcoRI bands (Fig. 3A, lanes 5 to 12; compare $-$ and $+$ T4 endo V) indicate that repair occurs in the WT but not in the $rad4\Delta$ cells. Quantitative analyses of the data reveal that in the WT, ~60% of the CPDs are removed after 4 h and that NER occurs at a uniform and low rate (Fig. 3B, WT). Very little or no repair was measured in the IS of the $rad4\Delta$ cells (Fig. 3B, $rad4\Delta$). Similar experiments were carried out with the $rad34\Delta$ and $rad4\Delta$ $rad34\Delta$ cells. The changes in signal intensities of the EcoRI bands (Fig. 3A, $rad34\Delta$; compare $-$ and $+$ T4 endo V in lanes 5 to 12) indicate that repair occurs in the $rad34\Delta$ cells but not in the double mutant (Fig. 3A, $rad4\Delta$ $rad34\Delta$). Quantitative analyses show that in the $rad34\Delta$ cells, ~60% of the CPDs are removed after 4 h and, similar to that of the WT, at a uniform and low rate (Fig. 3B, $rad34\Delta$). Again, very little or no repair was measured in the IS of the $rad4\Delta$ $rad34\Delta$ cells (Fig. 3B; $rad4\Delta$ $rad34\Delta$).

Rad4p-independent TC-NER starts 40 bases downstream of the transcription initiation site and is faster than that in the WT. To examine the role of Rad4p in more detail, we analyzed repair at nucleotide resolution (50). This enabled us to define where Rad4p is the determinant for NER, around the promoter and the first ~400 bases of the coding region. Figure 4 shows typical phosphor images of gels showing CPD repair in the TS (Fig. 4A) and NTS (Fig. 4B) of rDNA in the WT, $rad4\Delta$, and $rad34\Delta$ strains. The top band of each gel represents the whole HhaI restriction fragment (768 bp) (Fig. 1A, H_1 to H_2), free of CPDs, while each band below indicates the presence of a CPD at a single nucleotide position. The intensity of the bands reflects the frequency of lesions either at individual sites or in polypyrimidine tracts. A strong band indicates a high frequency of CPDs, and a fast disappearance of a band after repair time indicates fast repair. The quantified data are reported in Fig. 4C, where the time for removing 50% of the initial CPDs at each site ($T_{50\%}$) is plotted over ~500 bp of rDNA. Data points correspond either to a single CPD between adjacent pyrimidines or to clusters of CPDs that are formed at close proximity.
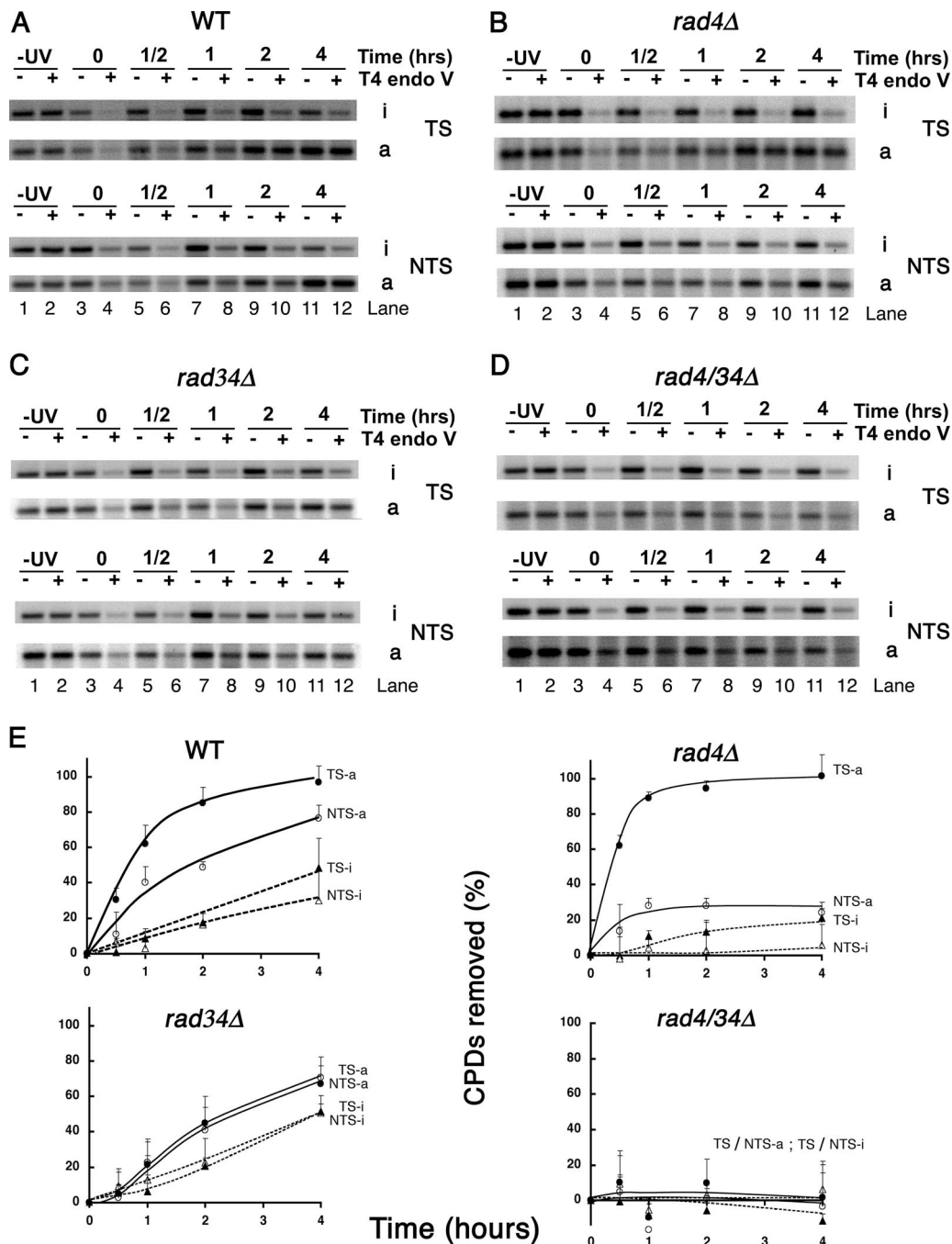
FIG. 2. Repair of individual DNA strands in the coding regions of active and inactive rDNA. Nuclei were isolated from unirradiated cells (−UV, lanes 1 and 2) and from cells that were irradiated at 180 J/m² (lanes 3 to 12). WT (A), *rad4Δ* (B), *rad34Δ* (C), and *rad4Δ rad34Δ* (D) cells were harvested at the times indicated (h). Nuclei were digested with EcoRI, and their DNA was isolated and redigested with NheI. DNA samples, mock treated or treated with T4 endo V (denoted by − and +, respectively), were separated on 1% alkaline agarose gels and blotted and hybridized with strand-specific riboprobes-A (see Fig. 1A). Upper panels show TS and lower panels show NTS. To conserve space, the central portion of each gel, separating the inactive (i) rDNA from the active (a) rDNA is not shown (examples of complete gels can be seen in reference 10). (E) Quantification of phosphor images. Data are from active rDNA (circles) and inactive rDNA (triangles). Filled and open symbols represent data from the TS and NTS, respectively. Data are the means ± 1 standard deviation of four independent experiments.

In the rDNA promoter of the WT, repair for the TS is generally slow and, upstream of position −20, the $T_{50\%}$ for most of the CPDs is over 5 h. A group of CPDs around position −10 is repaired faster, with a $T_{50\%}$ of ~3 h. Inside the coding region, from positions +5 to +34, repair slows down, with a $T_{50\%}$ of 3 to ~6 h. The next cluster of CPDs, downstream of position +40, is repaired rapidly, with a $T_{50\%}$ of less than 1 h. Fast repair occurs throughout the rest of the coding region examined, with $T_{50\%}$ measurements ranging from 0.5 to 2.5 h. Conversely, repair in the NTS is generally slow, with $T_{50\%}$
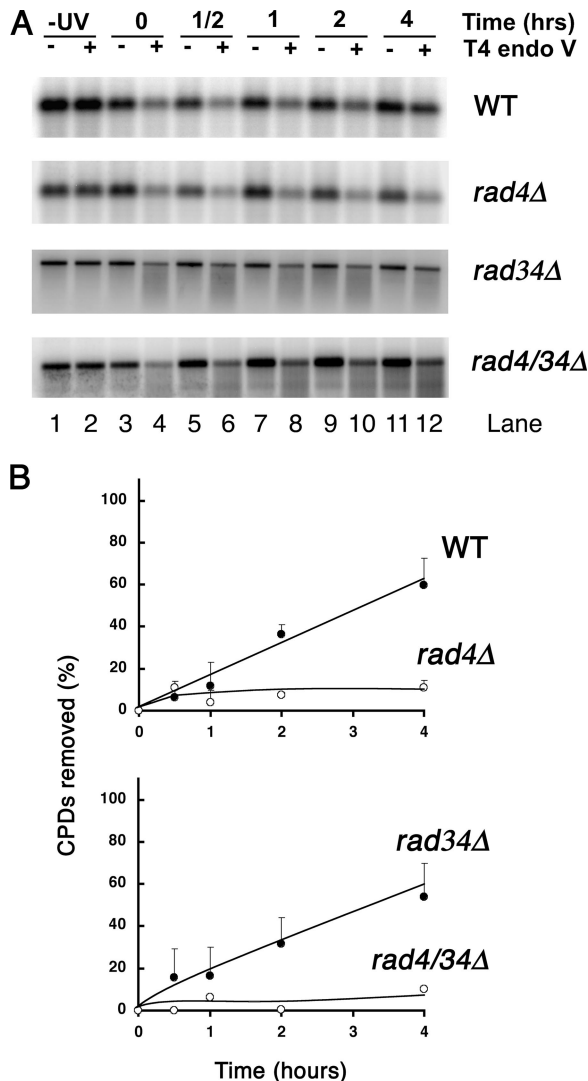
A

B

FIG. 3. Repair of CPDs in the IS. Cells were irradiated, and their DNA was prepared as described in the legend to Fig. 1B. After DNA separation on 1% alkaline agarose gel electrophoresis and blotting, filters were hybridized with random primer-labeled probe B. (A) Representative phosphor images for the WT, rad4Δ, rad34Δ, and rad4Δ rad34Δ cells. (B) Quantification of phosphorimager data. Data are the means ± 1 standard deviation of three independent experiments for the WT, rad4Δ and rad34Δ cells. For the rad4Δ rad34Δ cells, data are the means of two independent experiments.

measurements of over 3.5 h for all CPDs. This shows that strand-specific repair occurs in the promoter region and that TC-NER starts downstream of position +40. Analysis of the rad4Δ mutant shows that there is no repair in both DNA strands of the promoter and of the first 40 nucleotides in the coding region. However, beginning at position +40 and proceeding downstream, repair of CPDs in the TS is faster than that in the WT ($T_{50\%}$ of ~0.5 h for most sites), corroborating the data shown in Fig. 2E (rad4Δ). These results indicate that strand-specific repair between positions −10 and +34 requires Rad4p and that TC-NER from position +40 onward occurs in the absence of Rad4p.

Rad34p is required for Rad4p-independent TCR of rDNA. In the rad34Δ mutant, repair of CPDs in the TS and upstream of position −20 is slow. Like the repair rate measured in the WT, the $T_{50\%}$ in this region of the rDNA promoter is more than 5 h. Also, the repair rates in the TS between positions −10 and +34 are similar to those of the WT. Thus, strand-specific repair around the transcription initiation site requires Rad4p but is independent of Rad34p. Downstream of position +40, repair in rad34Δ is considerably slower (most of the $T_{50\%}$ are 6 h) than in the WT and rad4Δ mutant ($T_{50\%}$ of less than 1 h). These analyses of repair at the nucleotide level complement the data presented in Fig. 2E and show that Rad34p is necessary for TC-NER that starts around nucleotide +40. Repair of the NTS in the rad34Δ strain is homogenously slower than in the WT. We note that some CPDs are repaired in the rad34Δ mutant as measure by the T4 endo V/Southern blot assays. This is not necessarily found by the high-resolution analyses, as the plot shows $T_{50\%}$ of CPDs, irrespective of the amount of damage induced at any given CPD site. Moreover, high-resolution mapping of CPD removal was analyzed for each single nucleotide (or small groups of polypyrimidine tracts) in the first 502 bp of the rDNA-coding region. In contrast, repair rates measured by the T4 endo V/Southern blot assays (Fig. 2E) reflect the average repair rate of all CPDs within the large central portion of the rDNA-coding region (either 2.9 or 4.4 kb).

DISCUSSION

The separation of active and inactive rDNA populations, together with the repair data measured at the nucleotide level, have provided novel information about the roles of the Rad4 and Rad34 proteins. It was previously shown that in the rad4Δ cells, ~60% of CPDs are removed from the TS of total rDNA, whereas little or no repair occurs in the rest of the genome, including the NTS of total rDNA. These results were not fully explained since the assays used could not discriminate between active and inactive rDNA (59). We reexamined repair in total rDNA (Fig. 1B) and, in parallel, monitored repair in the active and inactive rDNA fractions (Fig. 2). Our results show that ~60% of CPDs removed from the TS of total rDNA correspond to the average of repair measured in the TS of active rDNA (100% of CPDs removed) and in the TS of inactive rDNA (less than 15% of CPDs removed). Therefore, in the rad4Δ cells, the TS of active rDNA is fully repaired, and almost no repair occurs in the TS of inactive rDNA. Interestingly, the TS of active rDNA is repaired faster in the rad4Δ cells than in the WT (Fig. 2E and 4C). Since, in the rad4Δ cells, NER is inoperative for most of the genome, very fast repair of the TS of active rDNA could reflect the extra availability of NER factors to repair rDNA. Also, the results in Fig. 2 show that both TC-NER and GG-NER participate in the removal of CPDs from the TS of active rDNA. In fact, in the absence of Rad34p, TC-NER is abolished, and only GG-NER is operative, and the two strands of active rDNA are equally and slowly repaired. On the other hand, in the rad4Δ cells GG-NER is abolished, and TC-NER is the only pathway that repairs the TS of active rDNA, which could also explain the very fast removal of CPDs from the TS. Yet, GG-NER is the main pathway that repairs the NTS of active rDNA and both DNA strands of
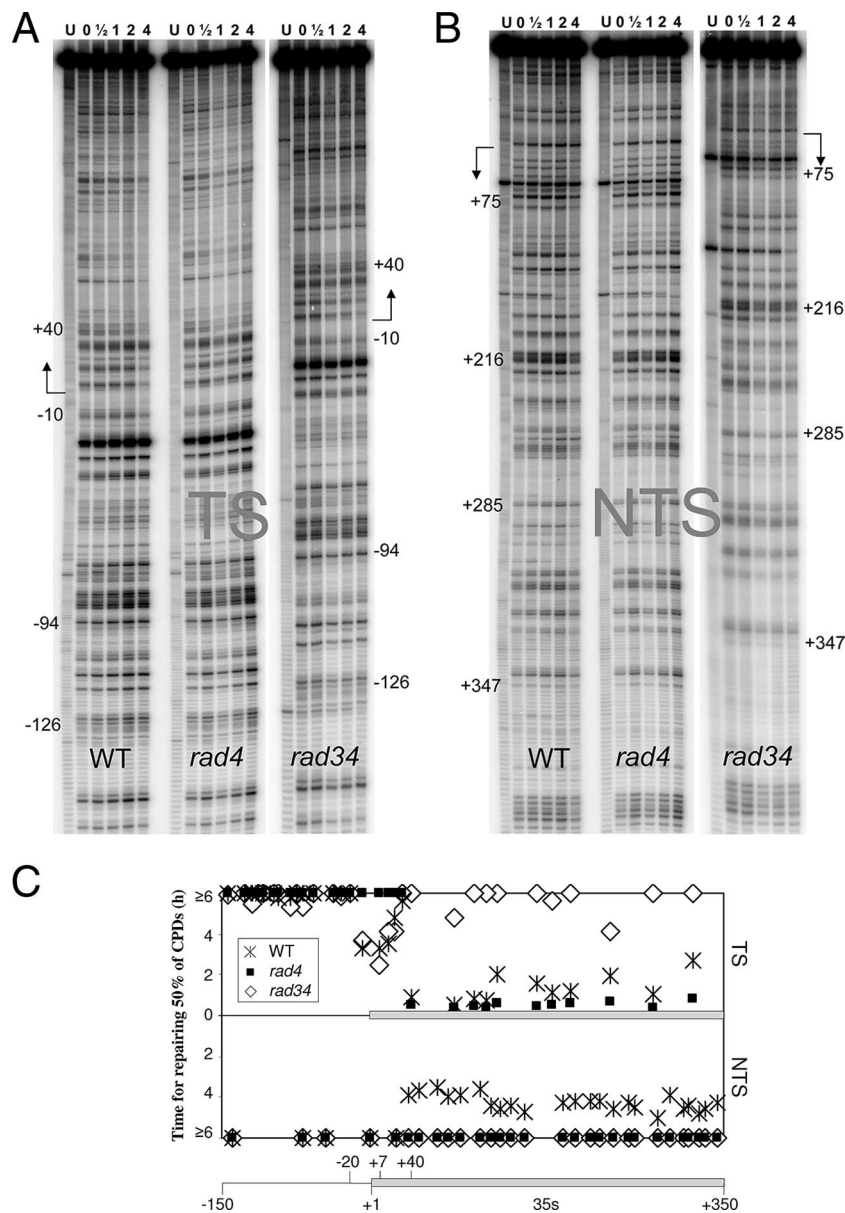
FIG. 4. Repair of CPDs in rDNA at nucleotide resolution. (A) Typical sequencing gels depicting repair of CPDs in the TS of the HhaI restriction fragment in WT, rad4Δ, and rad34Δ cells. U, DNA extracted from nonirradiated cells; 0, DNA extracted from cells immediately after UV (180 J/m²) exposure or after 0.5 1, 2, and 4 h of repair. The arrow indicates the direction of transcription and the initiation site. The numbers refer to the nucleotide positions related to the transcription initiation site (+1). (B) Typical sequencing gels depicting repair of CPDs in the NTS of HhaI restriction fragment in the WT, rad4Δ, and rad34Δ cells. (C) Repair is presented as the time (h) needed to remove 50% of CPDs at a given site in the HhaI fragment for the WT, rad4Δ and rad34Δ cells. Quantification of gels as shown in panels A and B enabled the calculation of $T_{50\%}$ for single or clustered CPDs with similar repair rates, as described in reference 50. The $T_{50\%}$ values for slowly repaired CPDs and nonrepaired CPDs ($T_{50\%} \geq 6$ h) are shown at the same level (6 h). The map represents the ~500-bp HhaI fragments comprising the rDNA promoter and the first ~350 bp of the coding region. The numbers indicate the nucleotide positions related to the transcription initiation site (+1).

inactive rDNA and is largely unaffected in the rad34Δ cells. As expected, no repair occurs when both pathways are abolished (e.g., the rad4Δ rad34Δ strain). Alternatively, very fast repair of the TS of active rDNA in the rad4Δ cells could be explained by Rad23p being essential for repairing CPDs in the rDNA locus (59) and by its capability of binding both Rad4p and Rad34p (18). In the absence of Rad4p, more Rad23p molecules would be available to form the active complex Rad23/Rad34p. However, the cellular ratio among Rad4p:Rad34p:Rad23p is 10:1:

140 (http://yeastgfp.ucsf.edu), which does not support the hypothesis that the amount of Rad23p is a limiting factor.

It was suggested that Rad34p could be involved in TC-NER as Rad34p takes part in repair of the bottom strand (14). Our results definitively show that Rad34p contributes to NER, mostly in the TS of active rDNA or TC-NER of RNAPI (Fig. 2E, rad34Δ). Moreover, examination of NER at the nucleotide level shows the presence of TC-NER downstream of nucleotide +40 (Fig. 4C). Also, past nucleotide +40, repair of the TS

is considerably slower in the *rad34Δ* strain than in the WT. These results demonstrate that Rad34p is essential for TC-NER and that TC-NER starts ~40 nucleotides downstream of nucleotide +1. Around the transcription initiation site (between nucleotides −10 and +34), repair is slow in the TS and very slow in the NTS, in both the WT and *rad34Δ* cells. In the *rad4Δ* strain, analyses of NER at the nucleotide level substantiate the existence of very fast repair in the TS of the coding region. In these cells, there is no repair in the NTS of the coding region, in both DNA strands of the promoter and between rDNA units. Hence, strand-specific repair between positions −10 and +34 requires Rad4p but not Rad34p, and TC-NER from position +40 onward occurs in the absence of Rad4p but requires Rad34p.

Rad4p is necessary for repair of RNAPII-transcribed genes, whereas Rad34 is not (14). Here we show that Rad4p is essential for repair in nontranscribed regions and at the transcription initiation site, whereas Rad34p is not, and that Rad34p is required for TC-NER of the immediate downstream region, where Rad4p has no role. Thus, although Rad4p and Rad34p share sequence homology (18, 31), their roles in repair are by and large distinct and complementary. However, we cannot completely exclude the possibility that Rad4p and Rad34p have at least small overlapping functions. In fact, in *rad4Δ* cells, ~20% of CPDs are repaired from the NTS of active rDNA, and Rad34p could be responsible for this small NER activity. This is substantiated by the data showing that the repair of the same NTS of active rDNA is ~15% less effective in the *rad34Δ* cells than in WT cells (Fig. 2E). Another possible explanation for the low (but statistically significant) level of repair in the NTS of the *rad4Δ* active rDNA could be the occurrence of transcription in the opposite direction. However, in the yeast strains used for this study (*SIR2*^{+}, *NRD1*^{+}, *NAB3*^{+}, and *SEN1*^{+}), there is no transcription of rDNA running in the opposite direction (56). Moreover, we could not find antisense rRNA corresponding to the central portion of rDNA, which is the region where we have measured DNA repair (data not shown).

The distinct and complementary participation of Rad4p and Rad34p could reflect the state of the RNAPI transcription complex. Namely, transcription initiation requires (i) melting of DNA to form an open complex, (ii) formation of the first few phosphodiester bonds, (iii) beginning of RNAPI movement, (iv) clearance of the promoter, and (v) formation of a steady-state ternary elongation complex. The melted DNA region starts upstream of the transcription initiation site (at nucleotide −7), expanding downstream and forming a transcription bubble of ~19 bp. Furthermore, RNAPI covers ~26 bp and clears the promoter at about nucleotide +12 (27). Thus, it is tempting to suggest that Rad4p (or GG-NER) is needed to repair rDNA from upstream of the transcription initiation site to the promoter clearance step, whereas Rad34p (or TC-NER) is needed during transcription elongation. However, the specific role of Rad34p during TC-NER of RNAPI remains unknown. Perhaps it could promote repair at sites where RNA polymerases are arrested by DNA lesions, similar to the roles proposed for Rad26p (and for the human homologue CSB) during TC-NER of RNAPII-transcribed genes (29). It should be noted that the CSB protein is also a component of RNAPI transcription in human cell lines, and, thus, CSB/Rad26p could
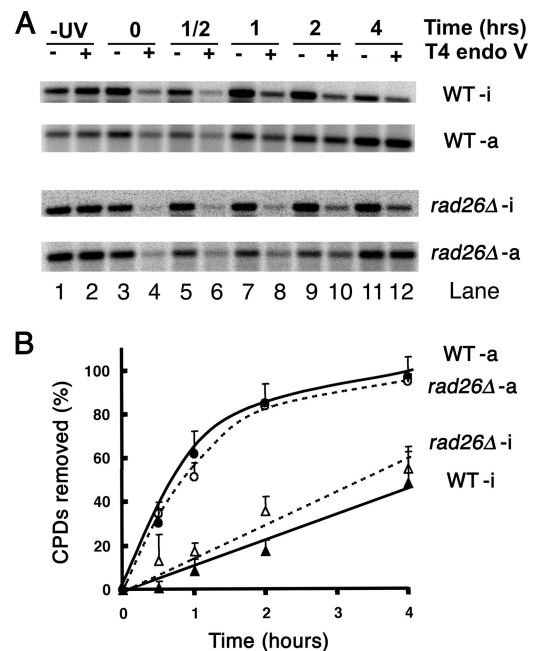

FIG. 5. Repair of the TS in the coding regions of inactive and active rDNA, from WT and *rad26Δ* cells. (A) Nuclei were isolated from unirradiated and irradiated cells and digested with EcoRI as described in the legend to Fig. 2. Their DNA was isolated, redigested with NheI, mock treated or treated with T4 endo V (denoted by − and +, respectively), separated on a 1% alkaline agarose gel, blotted, and hybridized with strand-specific riboprobes-A (see the legend to Fig. 1A). i, inactive rDNA; a, active rDNA. (B) Quantification of phosphor images. Data are from active rDNA (circles) and inactive rDNA (triangles). Filled and open symbols represent data from the WT and *rad26Δ* cells, respectively. Data are the means ± 1 standard deviation of four independent experiments.

participate in NER of rRNA genes (5). Although it is not known whether Rad26p promotes RNAPI transcription in yeast, an early study considered the possibility that Rad26p might participate in the repair of total rDNA. It was reported that Rad26p is not involved in NER of total rDNA (59). However, in that same study TC-NER could not be measured in total rDNA of WT yeast, leaving open the possibility that Rad26p could contribute to the repair of the TS of active rDNA. Accurate measurements for DNA repair in the TS of both active and inactive rDNA, in the WT and *rad26Δ* cells, are shown in Fig. 5. Clearly, the data presented here prove that Rad26p does not participate in TC-NER of RNAPI-transcribed rDNA.

Chromatin, chromatin remodeling, and histone modification modulate NER activity (51, 52, 54, 64, 66). We exploited the yeast rDNA locus and its two distinct structures to follow NER in chromatin (6). Canonical nucleosomes are not present in the coding regions of active rRNA genes, which are loaded with RNAPI molecules to a ratio of one RNAPI for every 100 bp (i.e., about two RNAPI molecules for every nucleosome DNA length) (37). Conversely, nucleosomes are found on the same coding DNA sequences in silent genes and on the majority of DNA between rDNA units (IS) (12, 30, 47). We observed that in WT cells, nucleosomes hamper NER, since the NTS of active rDNA is repaired faster than both DNA strands of

inactive rDNA. Moreover, the kinetics of NER for active and inactive rDNA are different, as follows: fast at the beginning and slow at the end in the coding region of active (nonnucleosome) rDNA and uniformly slow in the coding region of inactive (nucleosome) rDNA. Similarly, uniform and low repair rates occur in the IS (Fig. 3). It is hypothesized that XPC makes compact chromatin accessible to NER. However, in the *rad34Δ* strain, repairs of CPDs from inactive rDNA and from the IS are unaffected. Thus, although Rad34p shares sequence homology with XPC and Rad4p, it does not promote NER in arrays of nucleosomes. Even though the components of active (nonnucleosome) rDNA chromatin are unknown (53), active rDNA is largely devoid of histones, which are replaced with the protein Hmo1 (36). Hmo1p binds to the promoter and throughout the entire rDNA-coding region and enhances transcription (17, 25). Moreover, the initiation of rDNA transcription begins with the assembly of upstream activating factor (UAF), core factor (CF), TATA-box binding protein (TBP), Rrn3p, and RNAPI on the upstream element and core promoter (Fig. 1A, lower panel [39]). Like NER (see description above), photolyase repair of CPDs in the yeast rDNA sequences is hindered by the presence of nucleosomes, and photoreactivation experiments confirmed the presence of CF and UAF at rDNA regulatory regions (32, 33). In WT cells, NER is slow over the entire RNAPI promoter and downstream of the transcription initiation site up to nucleotide +34 (Fig. 4C). Similarly, NER is slow in the RNAPII and -III promoters (9, 50). Thus, it is likely that RNA polymerase transcription initiation complexes obstruct the multienzymatic mechanism of NER, which covers about 30 nucleotides around the damaged site (62). In *rad4Δ* cells, the rDNA promoter, the inactive (nucleosome) rDNA coding region, and the IS are not repaired, whereas the TS of active (nonnucleosome) rDNA is repaired. Since Rad4p copurifies with the SWI/SNF chromatin-remodeling complex, it is suggested that it could recruit SWI/SNF to enhance repair in chromatin (20). However, in *rad4Δ* cell repair of the NTS of active (nonnucleosome) rDNA is severely reduced. Hence, the interpretation for an apparent role of Rad4p in repair of nucleosomes remains unclear, at least in the rDNA locus.

In conclusion, with this study, we have added important information about the functions of the XPC family of proteins in NER. The current knowledge of the participation of Rad4p and Rad34p in NER of rDNA has been taken to the next level, and we provided insights into their roles during repair of nucleosome versus nonnucleosome rDNA and in regulatory protein/DNA complexes at rDNA regulatory regions. Our results indicate that, although Rad4p and Rad34p share sequence homology, their roles in repair of rDNA are distinct. Rad4p is essential for repair in nontranscribed regions and at the transcription initiation site, whereas Rad34p is not; Rad34p is required for TC-NER of the immediate downstream region, where Rad4p has no role.

REFERENCES

1. **Baker-Brachmann, C., A. Davies, G. J. Cost, E. Caputo, J. Li, P. Hieter, and J. D. Boeke.** 1998. Designer deletion strains derived from *Saccharomyces cerevisiae* S288C: a useful set of strains and plasmids for PCR-mediated gene disruption and other applications. Yeast **14:**115–132.
2. **Bardwell, A. J., L. Bardwell, N. Iyer, J. Q. Svejstrup, W. J. Feaver, R. D. Kornberg, and E. C. Friedberg.** 1994. Yeast nucleotide excision repair proteins Rad2 and Rad4 interact with RNA polymerase II basal transcription factor b (TFIIH). Mol. Cell. Biol. **14:**3569–3576.
3. **Bohr, V. A., and P. C. Hanawalt.** 1985. DNA repair in an active gene: removal of pyrimidine dimers from the DHFR gene of CHO cells is much more efficient than in the genome overall. Cell **40:**359–369.
4. **Bordi, L., F. Cioci, and G. Camilloni.** 2001. In vivo binding and hierarchy of assembly of the yeast RNA polymerase I transcription factors. Mol. Biol. Cell **12:**753–760.
5. **Bradsher, J., J. Auriol, L. Proietti de Santis, S. Iben, J.-L. Vonesch, I. Grummt, and J.-M. Egly.** 2002. CSB is a component of RNA pol I transcription. Mol. Cell **10:**819–829.
6. **Conconi, A.** 2005. The yeast rDNA locus: a model system to study DNA repair in chromatin. DNA Rep. **4:**897–908.
7. **Conconi, A., V. A. Bespalov, and M. J. Smerdon.** 2002. Transcription-coupled repair in RNA polymerase I-transcribed genes of yeast. Proc. Natl. Acad. Sci. USA **99:**649–654.
8. **Conconi, A., V. A. Bespalov, D. Fahy, and M. J. Smerdon.** 2005. DNA repair in RNA polymerase I transcribed genes, p. 123–147. *In* E. Sage, R. Drouin, and M. Rouabhia (ed.), From DNA photolesions to mutations, skin cancer and cell death: comprehensive series in photochemical and photobiological sciences. RSC Publishing, London, United Kingdom.
9. **Conconi, A., X. Liu, L. Koriazova, E. J. Ackerman, and M. J. Smerdon.** 1999. Tight correlation between inhibition of DNA repair in vitro and transcription factor IIIA binding in a 5S ribosomal RNA gene. EMBO J. **18:**1387–1396.
10. **Conconi, A., M. Paquette, D. Fahy, V. A. Bespalov, and M. J. Smerdon.** 2005. Repair-independent chromatin assembly onto active ribosomal genes in yeast after UV irradiation. Mol. Cell. Biol. **25:**9773–9783.
11. **Conconi, A., R. M. Widmer, T. Koller, and J. M. Sogo.** 1989. Two different chromatin structures coexist in ribosomal RNA genes throughout the cell cycle. Cell **57:**753–776.
12. **Dammann, R., R. Lucchini, T. Koller, and J. M. Sogo.** 1993. Chromatin structure and transcription of rDNA in yeast Saccharomyces cerevisiae. Nucleic Acids Res. **21:**2331–2338.
13. **Dammann, R., R. Lucchini, T. Koller, and J. M. Sogo.** 1995. Transcription in the yeast rRNA gene locus: distribution of the active gene copies and chromatin structure of their flanking regulatory sequences. Mol. Cell. Biol. **15:**5294–5303.
14. **den Dulk, B., J. A. Brandsma, and J. Brouwer.** 2005. The Rad4 homologue YDR314C is essential for strand-specific repair of RNA polymerase I-transcribed rDNA in *Saccharomyces cerevisiae*. Mol. Microbiol. **56:**1518–1526.
15. **den Dulk, B., S. M. Sun, M. de Ruijter, J. A. Brandsma, and J. Brouwer.** 2006. Rad33, a new factor involved in nucleotide excision repair in *Saccharomyces cerevisiae*. DNA Rep. **5:**683–692.
16. **Friedberg, E. C., G. C. Walker, W. Siede, R. D. Wood, R. A. Schultz, and T. Ellenberger.** 2006. DNA repair and mutagenesis. ASM Press, Washington, DC.
17. **Gadal, O., S. Labarre, C. Boschiero, and P. Thuriaux.** 2002. Hmo1, an HMG-box protein, belongs to the yeast ribosomal DNA transcription system. EMBO J. **21:**5498–5507.
18. **Gavin, A. C., M. Bosche, R. Krause, P. Grandi, M. Marzioch, A. Bauer, J. Schultz, et al.** 2002. Functional organization of the yeast proteome by systematic analysis of protein complexes. Nature **415:**141–147.
19. **Gillette, T. G., S. Yu, Z. Zhou, R. Waters, S. A. Johnson, and S. H. Reed.** 2006. Distinct functions of ubiquitin-proteasome pathway influence nucleotide excision repair. EMBO J. **25:**2529–2538.
20. **Gong, F., D. Fahy, and M. J. Smerdon.** 2006. Rad4-Rad23 interaction with SWI/SNF links ATP-dependent chromatin remodeling with nucleotide excision repair. Nat. Struct. Mol. Biol. **13:**902–907.
21. **Grummt, I., and C. S. Pikaard.** 2003. Epigenetic silencing of RNA polymerase I transcription. Nat. Rev. Mol. Cell Biol. **4:**641–649.
22. **Guzder, S. N., V. Bailly, P. Sung, L. Prakash, and S. Prakash.** 1995. Yeast DNA repair protein RAD23 promotes complex formation between transcription factor TFIIH and DNA damage recognition factor RAD14. J. Biol. Chem. **270:**8385–8388.
23. **Guzder, S. N., Y. Habraken, P. Sung, L. Prakash, and S. Prakash.** 1995. Reconstitution of yeast nucleotide excision repair with purified rad proteins, replication protein A, and transcription factor TFIIH. J. Biol. Chem. **270:**12973–12976.
24. **Guzder, S. N., P. Sung, L. Prakash, and S. Prakash.** 1998. Affinity of yeast nucleotide excision repair factor 2, consisting of the Rad4 and Rad23 proteins, for ultraviolet damaged DNA. J. Biol. Chem. **273:**31541–31546.
25. **Hall, D. B., J. T. Wade, and K. Struhl.** 2006. An HMG protein, Hmo1, associates with promoters of many ribosomal protein genes and throughout

the rRNA gene locus in *Saccharomyces cerevisiae*. Mol. Cell. Biol. **26:**3672–3679.

26. **Hara, R., J. Mo, and A. Sancar.** 2000. DNA damage in the nucleosome core is refractory to repair by human excision nuclease. Mol. Cell. Biol. **20:**9173–9181.

27. **Kahl, B. F., H. Li, and M. R. Paule.** 2000. DNA melting and promoter clearance by eukaryotic RNA polymerase I. J. Mol. Biol. **299:**75–89.

28. **Jansen, L. E. T., R. A. Verhage, and J. Brouwer.** 1998. Preferential binding of yeast Rad4–Rad23 complex to damaged DNA. J. Biol. Chem. **273:**33111–33114.

29. **Lainé, J.-P., and J.-M. Egly.** 2006. When transcription and repair meet: a complex system. Trends Genet. **22:**430–436.

30. **Lucchini, R., and J. M. Sogo.** 1998. The dynamic structure of ribosomal RNA gene chromatin, p. 255–276. *In* M. R. Paule (ed.), Transcription of ribosomal genes by eukaryotic RNA polymerase I. Springer-Verlag, New York, NY.

31. **Marti, T. M., C. Kunz, and O. Fleck.** 2003. Repair of damaged and mismatched DNA by the XPC homologues Rhp41 and Rhp42 of fission yeast. Genetics **164:**457–467.

32. **Meier, A., and F. Thoma.** 2005. RNA polymerase I transcription factors in active yeast rRNA gene promoters enhance UV damage formation and inhibit repair. Mol. Cell. Biol. **25:**1586–1595.

33. **Meier, A., M. Livingstone-Zatchej, and F. Thoma.** 2002. Repair of active and silenced rDNA in yeast. J. Biol. Chem. **277:**11845–11852.

34. **Mellon, I., V. A. Bohr, C. A. Smith, and P. C. Hanawalt.** 1986. Preferential DNA repair of an active gene in human cells. Proc. Natl. Acad. Sci. USA **83:**8878–8882.

35. **Mellon, I., G. Spivak, and P. C. Hanawalt.** 1987. Selective removal of transcription-blocking DNA damage from the transcribed strand of the mammalian *DHFR* gene. Cell **51:**241–249.

36. **Merz, K., M. Hondele, H. Goetze, K. Gmelch, U. Stoeckl, and J. Griesenbeck.** 2008. Actively transcribed rRNA genes in S. cerevisiae are organized in a specialized chromatin associated with the high-mobility group protein Hmo1 and are largely devoid of histone molecules. Genes Dev. **22:**1190–1204.

37. **Miller, O. L., Jr., and B. R. Beatty.** 1969. Visualization of nucleolar genes. Science **164:**955–957.

38. **Min, J.-H., and N. P. Pavletich.** 2007. Recognition of DNA damage by the Rad4 nucleotide excision repair protein. Nature **449:**570–576.

39. **Moss, T.** 2004. At the crossroads of growth control: making ribosomal RNA. Curr. Opin. Genet. Dev. **14:**210–217.

40. **Mu, D., D. S. Hsu, and A. Sancar.** 1996. Reaction mechanism of human DNA repair excision nuclease. J. Biol. Chem. **271:**8285–8294.

41. **Muller, M., R. Lucchini, and J. M. Sogo.** 2000. Replication of yeast rDNA initiates downstream of transcriptionally active genes. Mol. Cell **5:**767–777.

42. **Nomura, M.** 2001. Ribosomal RNA genes, RNA polymerases, nucleolar structures, and synthesis of rRNA in the yeast Saccharomyces cerevisiae. Cold Spring Harbor Symp. Quant. Biol. **66:**555–565.

43. **Prakash, S., and L. Prakash.** 2000. Nucleotide excision repair in yeast. Mutation Res. **451:**13–24.

44. **Reed, S. H., and T. G. Gillette.** 2007. Nucleotide excision repair and the ubiquitin proteasome pathway. Do all roads lead to Rome? DNA Rep. **6:**149–156.

45. **Smerdon, M. J., and F. Thoma.** 1990. Site-specific DNA repair at the nucleosome level in a yeast minichromosome. Cell **61:**675–684.

46. **Smith, J. S., E. Caputo, and J. D. Boeke.** 1999. A genetic screen for ribosomal DNA silencing defects identifies multiple DNA replication and chromatin-modulating factors. Mol. Cell. Biol. **19:**3184–3197.

47. **Sogo, J. M., and F. Thoma.** 2003. The structure of rDNA chromatin, p. 1–15. *In* M. O. J. Olson (ed.), The nucleolus. Kluwer Academic/Plenum Publishers, London, United Kingdom.

48. **Sugasawa, K., and F. Hanaoka.** 2007. Sensing of DNA damage by XPC/Rad4: one protein for many lesions. Nat. Struct. Mol. Biol. **14:**887–888.

49. Reference deleted.

50. **Teng, Y., S. Li, R. Waters, and S. H. Reed.** 1997. Excision repair at the level of the nucleotide in the Saccharomyces cerevisiae MFA2 gene: mapping of where enhanced repair in the transcribed strand begins or ends and identi-fication of only a partial rad16 requisite for repairing upstream control sequences. J. Mol. Biol. **267:**324–337.

51. **Teng, Y., H. Liu, H. W. Gill, Y. Yu, R. Waters, and S. H. Reed.** 2008. Saccharomyces cerevisiae Rad16 mediates ultraviolet-dependent histone H3 acetylation required for efficient global genome nucleotide-excision repair. EMBO Rep. **9:**97–102.

52. **Teng, Y., Y. Yu, and R. Waters.** 2002. The Saccharomyces cerevisiae histone acetyltransferase Gcn5 has a role in the photoreactivation and nucleotide excision repair of UV-induced cyclobutane pyrimidine dimers in the MFA2 gene. J. Mol. Biol. **316:**489–499.

53. **Toussaint, M., G. Levasseur, M. Tremblay, M. Paquette, and A. Conconi.** 2005. Psoralen photocrosslinking, a tool to study the chromatin structure of RNA polymerase I-transcribed ribosomal genes. Biochem. Cell Biol. **83:**449–459.

54. **Tremblay, M., M. Toussaint, A. D'Amours, and A. Conconi.** Nucleotide excision repair and photolyase repair of UV photoproducts in nucleosomes; assessing the existence of nucleosome and non-nucleosome rDNA chromatin *in vivo*. Biochem. Cell Biol., in press.

55. **van Gool, A. J., R. Verhage, S. M. A. Swagemakers, P. van de Putte, J. Brouwer, C. Troelstra, D. Bootsma, and J. H. J. Hoeijmakers.** 1994. RAD26, the functional *S. cerevisiae* homolog of the Cockayne syndrome B gene *ERCC6*. EMBO J. **13:**5361–5369.

56. **Vasiljeva, L., M. Kim, N. Terzi, L. M. Soares, and S. Buratowski.** 2008. Transcription termination and RNA degradation contribute to silencing of RNA polymerase II transcription within heterochromatin. Mol. Cell **29:**313–323.

57. **Venema, J., A. van Hoffen, V. Karcagi, A. T. Natarajan, A. A. van Zeeland, and L. H. F. Mullenders.** 1991. Xeroderma pigmentosum complementation group C cells remove pyrimidine dimers selectively from the transcribed strand of active genes. Mol. Cell. Biol. **11:**4128–4134.

58. **Venema, J., A. van Hoffen, A. T. Natarajan, A. A. van Zeeland, and L. H. F. Mullenders.** 1990. The residual repair capacity of xeroderma pigmentosum complementation group C fibroblasts is highly specific for transcriptionally active DNA. Nucleic Acids Res. **18:**443–448.

59. **Verhage, R. A., P. van de Putte, and J. Brouwer.** 1996. Repair of rDNA in *Saccharomyces cerevisiae*: *RAD4*-independent strand-specific nucleotide excision repair of RNA polymerase I transcribed genes. Nucleic Acids Res. **24:**1020–1025.

60. **Verhage, R. A., A.-M. Zeeman, N. De Groot, F. Gleig, D. Duong Bang, P. van de Putte, and J. Brouwer.** 1994. The *RAD7* and *RAD16* genes, which are essential for pyrimidine dimer removal from the silent mating type loci, are also required for repair of the nontranscribed strand of an active gene in Saccharomyces cerevisiae. Mol. Cell. Biol. **14:**6135–6142.

61. **Vogelauer, M., F. Cioci, and G. Camilloni.** 1998. DNA protein-interactions at the *Saccharomyces cerevisiae* 35 S rRNA promoter and in its surrounding region. J. Mol. Biol. **275:**197–209.

62. **Wakasugi, M., and A. Sancar.** 1998. Assembly, subunit composition, and footprinting of human DNA repair excision nuclease. Proc. Natl. Acad. Sci. USA **95:**6669–6674.

63. **Wang, Z., S. Wei, S. H. Reed, X. Wu, J. Q. Svejstrup, W. J. Feaver, R. D. Kornberg, and E. C. Friedberg.** 1997. The *RAD7*, *RAD16*, and *RAD23* genes of *Saccharomyces cerevisiae*: requirement for transcription-independent nucleotide excision repair in vitro and interactions between the gene products. Mol. Cell. Biol. **17:**635–643.

64. **Waters, R., and M. J. Smerdon.** 2005. Nucleotide excision repair in chromatin: searching for the key to enter. DNA Rep. **4(Suppl.):**853–950.

65. **Watkins, J. F., P. Sung, L. Prakash, and S. Prakash.** 1993. The *Saccharomyces cerevisiae* DNA repair gene RAD23 encodes a nuclear protein containing a ubiquitin-like domain required for biological function. Mol. Cell. Biol. **13:**7757–7765.

65a. **Yasuda, T., K. Sugasawa, Y. Shimizu, S. Iwai, T. Shiomi, and F. Hanaoka.** 2005. Nucleosomal structure of undamaged DNA regions suppresses the non-specific DNA binding of the XPC complex. DNA Rep. **4:**389–395.

66. **Yu, Y., Y. Teng, H. Liu, S. H. Reed, and R. Waters.** 2005. UV irradiation stimulates histone acetylation and chromatin remodeling at a repressed yeast locus. Proc. Natl. Acad. Sci. USA **102:**8650–8655.